Stable Lifting Construction of Non-Uniform Biorthogonal Spline Wavelets with Compact Support

Jan Maes *Adhemar Bultheel*

Report TW 437, October 2005

Katholieke Universiteit Leuven
Department of Computer Science
Celestijnenlaan 200A – B-3001 Heverlee (Belgium)

Stable Lifting Construction of Non-Uniform Biorthogonal Spline Wavelets with Compact Support

Jan Maes　　*Adhemar Bultheel*

Report TW 437, October 2005

Department of Computer Science, K.U.Leuven

Abstract

In this paper we use the lifting scheme to construct biorthogonal spline wavelet bases on regularly refined non-uniform grids. The wavelets have at least one vanishing moment and on each resolution level they form an L_2 Riesz basis. Furthermore we are interested in determining the exact range of Sobolev exponents for which the complete multilevel system forms a Riesz basis. Hereto we need to examine the smoothness of the dual scaling functions which involves investigation of the spectral properties of the associated transition operator. We provide several examples and discuss their stability. Furthermore we also give a strategy to construct biorthogonal spline wavelets on uniform grids.

Keywords : multiresolution analysis, biorthogonal wavelets, lifting, stability, elliptic variational problems
AMS(MOS) Classification : 65T60, 65D07, 65N30, 65F35

Stable Lifting Construction of Non-Uniform Biorthogonal Spline Wavelets with Compact Support

Jan Maes Adhemar Bultheel

October 2005

Abstract

In this paper we use the lifting scheme to construct biorthogonal spline wavelet bases on regularly refined non-uniform grids. The wavelets have at least one vanishing moment and on each resolution level they form an L_2 Riesz basis. Furthermore we are interested in determining the exact range of Sobolev exponents for which the complete multilevel system forms a Riesz basis. Hereto we need to examine the smoothness of the dual scaling functions which involves investigation of the spectral properties of the associated transition operator. We provide several examples and discuss their stability. Furthermore we also give a strategy to construct biorthogonal spline wavelets on uniform grids.

Keywords: multiresolution analysis, biorthogonal wavelets, lifting, stability, elliptic variational problems
AMS(MOS) Classification: 65T60, 65D07, 65N30, 65F35

1 Introduction

In recent years wavelets have become a well-appreciated discretization tool for solving elliptic variational problems, see e.g. [14, 10, 27, 19, 3, 6, 8]. Therefore, let us recall at first some properties of Galerkin discretizations of elliptic variational problems in a bounded domain and their relationship to the Riesz bounds of the underlying basis.

Let $\mathcal{H}$ be a Hilbert space with inner product $\langle\cdot,\cdot\rangle_{\mathcal{H}}$, and let $a(\cdot,\cdot)$ be a symmetric bilinear form such that $a(v,v)\sim\|v\|^2_{\mathcal{H}}$. We always mean by $A\sim B$ that A can be bounded above and below by constant multiples of B. Let $\mathcal{H}'$ denote the dual of $\mathcal{H}$. Consider the elliptic variational problem:

$$\begin{array}{c}\text{Given } f\in\mathcal{H}', \text{ find } u\in\mathcal{H} \text{ such that}\\ a(u,v)=f(v),\quad \forall v\in\mathcal{H}.\end{array}\tag{1}$$

Suppose V is a finite dimensional subspace of $\mathcal{H}$ with basis $\{B_j : j=1,\dots,N\}$. The Galerkin approximate solution $u_V=\sum_{j=1}^N c_jB_j$ is the unique solution of (1) with $\mathcal{H}$ replaced by V and it can be found by solving the linear system

$$\left(a(B_i,B_j)\right)_{i,j=1}^N\left(c_j\right)_{j=1}^N=\left(f(B_i)\right)_{i=1}^N.\tag{2}$$

The stiffness matrix $A=(a(B_i,B_j))_{i,j=1}^N$ for a typical nodal basis is ill-conditioned. Suppose that there exist constants $0<\gamma,\Gamma<\infty$ (Riesz bounds) such that

$$\gamma\sum_{j=1}^N|c_j|^2\le\|\sum_{j=1}^N c_jB_j\|^2_{\mathcal{H}}\le\Gamma\sum_{j=1}^N|c_j|^2,\tag{3}$$

then it is well-known that $\kappa(A)=\mathcal{O}(\Gamma/\gamma)$.

Let $\{B'_j : j=1,\dots,N\}$ be another basis for V. Then we can solve the linear system (2) with the basis functions B_j replaced by B'_j. The new system can be considered to arise from (2) by preconditioning. Hence, we are interested in basis functions B'_j for which $\kappa((a(B'_i, B'_j))_{i,j=1}^N) = \mathcal{O}(1)$.

In this paper we present a general construction method for wavelets on arbitrary domains that are suitable for preconditioning systems arising from elliptic variational problems. (We should note that a similar construction approach has been taken in [22] with applications in CAGD.) Section 2 gives a short overview of the principles of multiresolution analysis and lifting. Furthermore we explain how wavelets can be created on arbitrary domains and we discuss the design of the second lifting step, the update, in detail.

Section 3 contains theoretic material to investigate the Riesz basis property in the Sobolev space $H^s(\mathbb{R}^d)$ of a given hierarchical system. Crucial here is the derivation of the smoothness of the dual system. In order to be able to use Fourier techniques we will only consider the shift-dilation invariant setting of a multiresolution analysis, although realistic applications require other settings. Recently there has been a growing interest in the numerical computation of the smoothness of refinable functions (or function vectors), see e.g. [15, 30, 4] and references therein. However, a necessary condition in those papers is that the refinable functions (vectors) exist in L_2. The duals arising from the lifting scheme do not necessarily satisfy this condition [34]: it is possible that they only exist in distributional sense in L_2. This difficulty was dealt with by Lorentz and Oswald for the single function refinable case. In their paper [21] they provide sharp stability estimates for systems where the duals do not belong to L_2. Our main result in this section is Theorem 3.4 which extends this result to refinable function vectors.

In Section 4 we explicitly construct wavelets using the method from Section 2 and we investigate their stability using the theoretical framework from Section 3. Linear and quadratic spline wavelets are treated in one or two dimensions. Furthermore we numerically compare the constructed wavelet systems to standard finite element hierarchical bases. These numerical experiments confirm the theory.

To conclude the paper we briefly discuss a strategy to construct stable wavelets on uniform grids in Section 5. Using this strategy we find connections with other constructions in the literature.

2 Multiresolution decomposition on non-uniform grids

Let Ω be a bounded polygonal domain in $\mathbb{R}^d$ or $\mathbb{R}^d$ itself, with d the spatial dimension, and suppose that we are given a sequence $V_0 \subset V_1 \subset V_2 \subset \cdots \subset L_2(\Omega)$ of closed spline subspaces V_j of $L_2(\Omega)$ where each V_j has the form $V_j = \operatorname{span}\{\phi_{j,k} : k \in I_j\}$, and we refer to the spline functions $\phi_{j,k}$ as scaling functions. It will be convenient to use matrix notation. Define $\boldsymbol{\phi}_j$ as the row vector of all scaling functions $\phi_{j,k}$, $k \in I_j$. We assume that the scaling functions form an L_2 Riesz basis for V_j, i.e.

$$\|\boldsymbol{\phi}_j c\|_{L_2}^2 \sim c^T c. \tag{4}$$

Because the spaces V_j are nested there exists a subdivision matrix A_j such that $\boldsymbol{\phi}_j = \boldsymbol{\phi}_{j+1} A_j$. Such a subdivision matrix A_j can be written in block matrix form as $A_j = [O_j^T \quad N_j^T]^T$. We distinguish a part O_j that computes the coefficients of the basis functions on the finer grid associated with old vertices, and a part N_j that computes the coefficients of the basis functions on the finer grid associated with new vertices. Each space V_{j+1} contains splines on a finer grid than the previous coarser space V_j and therefore can describe more detail of a surface. These details are captured in an algebraic complement W_j such that $V_j \oplus W_j = V_{j+1}$. We will refer to the basis functions of W_j as wavelets and we denote $\boldsymbol{\psi}_j$ as the row vector of all wavelets that span W_j. The relation between $\boldsymbol{\psi}_j$ and $\boldsymbol{\phi}_{j+1}$ is given by a filter B_j, i.e. $\boldsymbol{\psi}_j = \boldsymbol{\phi}_{j+1} B_j$. In order to go from a coarse grid to a finer grid we use a regular refinement. This implies that there exists a constant ρ such that $\operatorname{diam}(\operatorname{supp} \phi_{j,k}) \sim \rho^{-j}$. Typically we have $\rho = 2$ (dyadic refinement).

The main idea is to start with a hierarchical basis and apply a local correction process on the scaling functions at each level in order to achieve certain stability properties (3) for the wavelets. This technique fits in the framework of both the lifting scheme [35] and the stable completion technique [2]. We split $\boldsymbol{\phi}_{j+1}$ in functions $\boldsymbol{\phi}_{j+1}^o$ associated with old grid points and functions $\boldsymbol{\phi}_{j+1}^n$ associated with new grid points when going from V_j to V_{j+1}, i.e. $\boldsymbol{\phi}_{j+1} = [\boldsymbol{\phi}_{j+1}^o \quad \boldsymbol{\phi}_{j+1}^n]$. The wavelets $\boldsymbol{\psi}_j$ are then initially defined as $\boldsymbol{\phi}_{j+1}^n$, and $B_j = [0 \quad I]^T$. We have now made a choice for the complement space W_j. This construction gives us a set of biorthogonal filter operators $\{A_j, B_j, \widetilde{A}_j, \widetilde{B}_j\}$ such that

$$[\boldsymbol{\phi}_j \quad \boldsymbol{\psi}_j] = \boldsymbol{\phi}_{j+1}[A_j \quad B_j], \qquad [\boldsymbol{\phi}_j \quad \boldsymbol{\psi}_j] \begin{bmatrix} \widetilde{A}_j \\ \widetilde{B}_j \end{bmatrix} = \boldsymbol{\phi}_{j+1}, \qquad \begin{bmatrix} \widetilde{A}_j \\ \widetilde{B}_j \end{bmatrix} [A_j \quad B_j] = I. \tag{5}$$

We also find dual scaling functions $\widetilde{\boldsymbol{\phi}}_j$ (that mainly consist of Dirac distributions and differential operators) and dual wavelets $\widetilde{\boldsymbol{\psi}}_j$ satisfying

$$[\widetilde{\boldsymbol{\phi}}_j \quad \widetilde{\boldsymbol{\psi}}_j] = \widetilde{\boldsymbol{\phi}}_{j+1}[\widetilde{A}_j^T \quad \widetilde{B}_j^T], \tag{6}$$

and they are biorthogonal in the sense that

$$\langle \widetilde{\phi}_{j,k}, \phi_{j,k'} \rangle = \delta_{k,k'}, \quad \langle \widetilde{\psi}_{j,m}, \psi_{j,m'} \rangle = \delta_{m,m'}, \quad \langle \widetilde{\phi}_{j,k}, \psi_{j,m} \rangle = 0, \quad \langle \widetilde{\psi}_{j,m}, \phi_{j,k} \rangle = 0. \tag{7}$$

As discussed before it can be desirable to have another complement space with certain properties. The new wavelet functions can be found by projecting the $\boldsymbol{\phi}_{j+1}^n$ into the desired complement space W^j along V_j, i.e. $\boldsymbol{\psi}_j = \boldsymbol{\phi}_{j+1}^n - \boldsymbol{\phi}_j C_j$. For each wavelet function there is a corresponding column in the lifting matrix C_j. The possibly nonzero entries in this column together will be called the stencil for that wavelet function. Note that if there are no zero entries in C_j, the wavelets will have the whole domain Ω as their support. The semiorthogonal construction orthogonalizes the new basis functions $\boldsymbol{\psi}_j$ to V_j. The lifting matrix C_j is found as the solution of the linear system $C_j = \langle \boldsymbol{\phi}_j, \boldsymbol{\phi}_j \rangle^{-1} \langle \boldsymbol{\phi}_j, \boldsymbol{\phi}_{j+1} \rangle$. Although this construction produces a stable multiscale basis, the wavelets are not practically useful because they are globally supported on Ω. However, the semiorthogonal lifting matrix has exponential off-diagonal decay [32, Lemma 5.2]. This motivates the use of local semiorthogonalization [22]. This construction method fixes the stencil in advance in order to have local support for the wavelet functions. Hence, a wavelet function on a new grid point is updated by the scaling functions of some neighbouring old grid points. The lifting matrix orthogonalizes the wavelets to their predefined set of scaling functions. Unfortunately this method does not yield stable multiscale bases. Hereto we need at least one vanishing moment, which implies that the dual scaling functions reproduce constants, a necessary condition for stability [31]. This leads to an overdetermined system because we do not have sufficient degrees of freedom. Our approach will be to construct the lifting matrix C_j as the least squares solution to this overdetermined system but we demand that the vanishing moment condition is fulfilled exactly. Once the lifting matrix is chosen we find a new set of biorthogonal filter operators $\{A_j, B_j - A_j C_j, \widetilde{A}_j + C_j \widetilde{B}_j, \widetilde{B}_j\}$ satisfying similar relations as above.

Theorem 2.1. *For each level j, the set of wavelets $\boldsymbol{\psi}_j$ forms an L_2 Riesz basis of W_j.*

Proof. Denote the one level wavelet transform filters as M_j. We show that $\|M_j\|_2, \|M_j^{-1}\|_2 = \mathcal{O}(1)$, uniformly in j. The filters M_j and M_j^{-1} can be factored as

$$M_j = \begin{bmatrix} O_j & 0 \\ 0 & I \end{bmatrix} \cdot \begin{bmatrix} I & 0 \\ N_j & I \end{bmatrix} \cdot \begin{bmatrix} I & -C_j \\ 0 & I \end{bmatrix}$$

and

$$M_j^{-1} = \begin{bmatrix} I & C_j \\ 0 & I \end{bmatrix} \cdot \begin{bmatrix} I & 0 \\ -N_j & I \end{bmatrix} \cdot \begin{bmatrix} O_j^{-1} & 0 \\ 0 & I \end{bmatrix}.$$

Hence it is sufficient to prove that $\|C_j\|_2, \|N_j\|_2, \|O_j\|_2, \|O_j^{-1}\|_2 = \mathcal{O}(1)$. Because of (4) one can show, using results from [2], that $\|N_j\|_2, \|O_j\|_2, \|O_j^{-1}\|_2 = \mathcal{O}(1)$. It remains to check whether the update is stable, i.e. $\|C_j\|_2 = \mathcal{O}(1)$. For band matrices with uniformly bounded bandwidth, the 1-norm and the 2-norm are equivalent uniformly in the dimensions of the matrix. Therefore it is sufficient to show that $\|C_j\|_1 \sim \max_{kl} |(C_j)_{kl}|$ is uniformly bounded. Let us focus on the update of a particular wavelet function $\psi_{j,k}$, where k represents a new grid point. The update involves a set of neighbouring scaling functions corresponding to old grid points. Let us denote these scaling functions by $\{\phi_{j,l} | l \in U_k\}$ with U_k an index set representing the old grid points and U_k satisfies by construction $\# U_k \lesssim 1$. Define the Gram matrix G as $G := (\langle \phi_{j,l_1}, \phi_{j,l_2} \rangle_{L_2})_{l_1,l_2 \in U_k}$. The update step solves the following overdetermined system

$$G \cdot c = b \quad \text{with} \quad b = (\langle \phi_{j,l}, \phi_{j+1,k} \rangle_{L_2})_{l \in U_k},$$

$$(\langle 1, \phi_{j,l} \rangle_{L_2})_{l \in U_k} \, c = \langle 1, \phi_{j+1,k} \rangle_{L_2}$$

in a least squares sense such that the vanishing moment condition is satisfied. Hence the column vector c, that is part of the lifting matrix C_j, satisfies

$$\begin{aligned} &G \cdot c = b + \epsilon \quad \text{with } \epsilon \text{ the least squares error}, \\ &(\langle 1, \phi_{j,l} \rangle_{L_2})_{l \in U_k} \, c = \langle 1, \phi_{j+1,k} \rangle_{L_2}. \end{aligned} \tag{8}$$

Suppose that $\{\phi^*_{j,l} | l \in U_k\}$ is a dual base for $\{\phi_{j,l} | l \in U_k\}$, i.e. $\langle \phi^*_{j,l_1}, \phi_{j,l_2} \rangle_{L_2} = \delta_{l_1,l_2}$, and suppose that $\phi^*_{j,l} =: \sum_{m \in U_k} b_{l,m} \phi_{j,m}$, then $G^{-1} = (b_{l,m})_{l,m \in U_k}$ and

$$\|\phi^*_{j,l}\|^2_{L_2} = \langle \phi^*_{j,l}, \phi^*_{j,l} \rangle_{L_2} = \left\langle \phi^*_{j,l}, \sum_{m \in U_k} b_{l,m} \phi_{j,m} \right\rangle_{L_2} = b_{l,l}. \tag{9}$$

From the L_2 stability of the scaling functions (4) it follows that $\sum_{m \in U_k} b^2_{l,m} \lesssim \|\phi^*_{j,l}\|^2_{L_2}$. So $\sum_{m \in U_k} b^2_{l,m} \lesssim b_{l,l}$ and we derive $b^2_{l,m} \lesssim b_{l,l}$. For $m = l$ this becomes $b_{l,l} \lesssim 1$. Combining these two yields

$$|b_{l,m}| \lesssim 1. \tag{10}$$

Due to (8)

$$\|c\|_\infty \leq \|G^{-1}\|_\infty (\|b\|_\infty + \|\epsilon\|_\infty). \tag{11}$$

Combining (9), (10) and (11) gives

$$\|c\|_\infty \lesssim \|\epsilon\|_\infty. \tag{12}$$

Suppose that we choose for the column vector c a solution in which all the entries c_l, $l \in U_k$, are equal to zero, except for one entry c_m, $m \in U_k$. From the vanishing moment condition we find $c_m = \langle 1, \phi_{j,m} \rangle^{-1}_{L_2} \langle 1, \phi_{j+1,k} \rangle_{L_2}$. Because the scaling functions form a Riesz basis of L_2 we have that $\langle 1, \phi_{j+1,k} \rangle_{L_2} \neq 0$ and $\langle 1, \phi_{j,m} \rangle_{L_2} \neq 0$, since a necessary condition for stability is the reproduction of polynomials of degree 0, see for instance [31]. In the shift invariant case this implies that the generator Φ satisfies $\langle 1, \Phi \rangle_{L_2} \neq 0$. Hence we immediately find $\langle 1, \phi_{j,m} \rangle_{L_2} \neq 0$ for all j and m by perturbation arguments. Then $\forall l \in U_k$, $|c_l| \lesssim 1$ independent of the level j, and $\|\epsilon\|_2 = \|G \cdot c - b\|_2 \lesssim 1$. Since the least squares method finds a c that minimizes $\|G \cdot c - b\|_2$, we have a contradiction if we suppose that $\|\epsilon\|_\infty \neq \mathcal{O}(1)$. Hence $\|\epsilon\|_\infty \lesssim 1$ and from (12) we get $\max_{kl} |(C_j)_{kl}| \lesssim 1$. □

Remark 2.2. Suppose that the scaling functions reproduce polynomials of degree $N - 1$. Then, using the local semiorthogonalization philosophy, we can demand up to N vanishing moments. If the update stencil is too small, the update coefficients in C_j might be unbounded. Simoens [32] gives examples of this phenomenon in the one-dimensional case and proposes a stabilized variant.

3 Stability over all levels

Theorem 2.1 does not imply that the multiscale basis $\bigcup_{j=0}^{\infty} \boldsymbol{\psi}_j$ is a uniformly stable Riesz basis for $L_2(\Omega)$. More generally, we are interested in the range of s for which the multiscale basis $\bigcup_{j=0}^{\infty} \boldsymbol{\psi}_j$ forms a Riesz basis for the Sobolev space $H^s(\Omega)$. The range of such s is determined by the Sobolev regularity of the scaling functions $\phi_{j,k}$ and the Sobolev regularity of the dual scaling functions $\widetilde{\phi}_{j,k}$. The Sobolev regularity or smoothness of an arbitrary function $f \in \Omega$ is measured by the critical exponent

$$s_f := \sup \{ s : f \in H^s(\Omega) \},$$

with $H^s(\Omega)$ the usual Sobolev spaces, see [1]. It is known (see [8]) that if $\phi_{j,k}, \widetilde{\phi}_{j,k} \in L_2(\Omega)$ have compact support, then the multiscale basis $\bigcup_{j=0}^{\infty} \boldsymbol{\psi}_j$ is a Riesz basis for $H^s(\Omega)$ for all s with $-s_{\widetilde{\Phi}} < s < s_\Phi$ and that this interval is sharp.

Realistic applications often require a multilevel basis on bounded domains Ω, such that the nested spaces V_j are not shift-dilation invariant. However, for our stability analysis we will assume a shift-dilation invariant setting for our multilevel basis, because this allows us to obtain estimates for the Sobolev regularity. We start with a geometric refinement described by the dilation matrix M which is of the form $M := \sigma I_d$, with σ an integer greater than 1, and denote $m := |\det M| = \sigma^d$. Let $\lambda_k + M\mathbb{Z}^d$ be the m distinct elements of $\mathbb{Z}^d/(M\mathbb{Z}^d)$, with $\lambda_0 = 0$. Define the sets

$$\Lambda := \{\lambda_k, k = 0, \dots, m-1\}, \quad \Lambda' := \Lambda \setminus \{\lambda_0\}.$$

In the most general case we find a multilevel system

$$\boldsymbol{\Psi} := \{\Phi(x-\alpha), m^{j/2}\Psi^\lambda(M^j x - \alpha), \alpha \in \mathbb{Z}^d, j = 0, 1, \dots,\ \lambda \in \Lambda'\}, \tag{13}$$

where

$$\Phi(x) = (\phi_1(x), \phi_2(x), \dots, \phi_r(x))^T, \quad \Psi^\lambda(x) = \left(\psi_1^\lambda(x), \psi_2^\lambda(x), \dots, \psi_r^\lambda(x)\right)^T$$

are $r \times 1$ function vectors on $\mathbb{R}^d$ that satisfy vector refinement equations of the form

$$\Phi(x) = \sum_{\alpha \in \mathbb{Z}^d} A_\alpha \Phi(Mx - \alpha), \tag{14}$$

$$\Psi^\lambda(x) = \sum_{\alpha \in \mathbb{Z}^d} A_\alpha^\lambda \Phi(Mx - \alpha), \tag{15}$$

with $\{A_\alpha\}_\alpha$ and $\{A_\alpha^\lambda\}_\alpha$ finitely supported sequences of $r \times r$ mask coefficient matrices.

Taking the Fourier transform of both sides of (14), we obtain

$$\widehat{\Phi}(\omega) = P(M^{-T}\omega)\widehat{\Phi}(M^{-T}\omega), \qquad \omega \in \mathbb{R}^d,$$

and

$$P(\omega) := m^{-1} \sum_{\alpha \in \mathbb{Z}^d} A_\alpha e^{-i\alpha\cdot\omega}, \qquad \omega \in \mathbb{R}^d,$$

is the symbol associated with (14). Here $P(\omega)$ is an $r \times r$ matrix function. Its entries are trigonometric polynomials with real coefficients. It is well-known that if $P(0)$ satisfies Condition E, i.e., 1 is a simple eigenvalue of $P(0)$ and all other eigenvalues of $P(0)$ lie inside the open unit disk, then there exists a unique compactly supported distributional solution vector $\Phi(u)$ satisfying (14) and $\Phi(0) = y_R$, with y_R (y_L) the normalized right (left) eigenvector of $P(0)$ associated with eigenvalue 1, see [28].

Without loss of generality we assume that the support of the symbol $P(\omega)$ is in the cube $[-N, N]^d$ for some fixed $N \geq 0$, so $A_\alpha = 0$ for all $\alpha \notin [-N, N]^d$. Let

$$K := \left(\sum_{j=1}^{\infty} M^{-j}([-2N, 2N]^d)\right) \cap \mathbb{Z}^d.$$

Define the torus $\mathbb{T} := [0, 2\pi]^d$ and let $C_0(\mathbb{T})^{r\times r}$ denote the space of all $r \times r$ matrix functions with trigonometric polynomial entries. For a given refinement equation with symbol $P(\omega) \in C_0(\mathbb{T})^{r\times r}$ we define the associated transition operator T_P on $C_0(\mathbb{T})^{r\times r}$ by

$$T_P H(\omega) := \sum_{k=0}^{m-1} P(M^{-T}(\omega + 2\pi\lambda_j))H(M^{-T}(\omega + 2\pi\lambda_j))P(M^{-T}(\omega + 2\pi\lambda_j))^*.$$

Define

$$\mathbb{H} := \{H(\omega) \in C_0(\mathbb{T}^d)^{r\times r} : H(\omega) = \sum_{\alpha \in K} H_\alpha e^{-i\alpha\cdot\omega}\},$$

then $\mathbb{H}$ is invariant under T_P. Furthermore we know from [13, 16] that the eigenfunctions of T_P corresponding to nonzero eigenvalues lie in $\mathbb{H}$. So it is sufficient to consider the restriction of T_P to $\mathbb{H}$ in order to study the eigenvalues and eigenfunctions of T_P.

Let us define the refinement operator R_P on $L_2(\mathbb{R}^d)^{r\times 1}$ by

$$R_P F := \sum_{\alpha\in\mathbb{Z}^d} A_\alpha F(M\cdot -\alpha),$$

then Φ solves (14) if $R_P\Phi = \Phi$. The cascade algorithm consists in the repeated application of R_P. If for some compactly supported initial $F \in L_2(\mathbb{R}^d)^{r\times 1}$ the cascade algorithm converges in the L_2 norm, then the vector function obtained in the limit is an $L_2(\mathbb{R}^d)^{r\times 1}$-solution of (14).

Theorem 3.1. *The cascade algorithm associated with the symbol $P(\omega)$ converges in the L_2 norm if and only if $P(\omega)$ satisfies sum rules of order 1, i.e.,*

$$y_L P(2\pi M^{-T}\lambda_k) = 0, \quad k = 1,\dots,m-1,$$

and the transition operator T_P satisfies Condition E.

Proofs can be found in [20, 31, 13]. Note that the requirement that $P(\omega)$ satisfies sum rules of order 1 is equivalent to the requirement that the shifts of the solution Φ of (14) reproduce polynomials of degree 0. The following theorem is the main result of the paper [15].

Theorem 3.2. *Let $\Phi \in L_2(\mathbb{R}^d)^{r\times 1}$ be the normalized solution of (14) with symbol $P(\omega)$. Suppose the highest degree of polynomials reproduced by Φ is $k-1$. Let*

$$E_k := \{\eta_l\sigma^{-\mu}, \overline{\eta}_l\sigma^{-\mu} : |\mu| < k, l = 2,\dots,r\} \cup \{\sigma^{-\mu} : |\mu| < 2k\},$$

with $\mu = (\mu_1,\dots,\mu_d) \in \mathbb{N}_0^d$, $\sigma^{-\mu} := \sigma^{-\mu_1}\cdots\sigma^{-\mu_d}$ and $\{\eta_1,\dots,\eta_r\} := \mathrm{spec}(P(0))$, where $\eta_1 = 1$ and $\eta_l \neq 1$ for $l = 2,\dots,r$. Define

$$\rho_k := \max\{|\nu| : \nu \in \mathrm{spec}(T_P|_{\mathbb{H}}) \setminus E_k\}.$$

Then

$$s_\Phi \geq -\frac{d}{2}\log_m \rho_k.$$

If Φ is L_2 stable then we have equality:

$$s_\Phi = -\frac{d}{2}\log_m \rho_k.$$

Suppose that the multilevel system (13) is a Riesz basis of $L_2(\mathbb{R}^d)$. Then equations (5) and (6) yield a dual system $\widetilde{\mathbf{\Psi}} := \{\widetilde{\Phi}(x-\alpha), m^{j/2}\widetilde{\Psi}^\lambda(M^j x-\alpha), \alpha\in\mathbb{Z}^d, j = 0,1,\dots,\ \lambda\in\Lambda'\}$ which is also a Riesz basis of $L_2(\mathbb{R}^d)$ satisfying (7). Furthermore

$$\widetilde{\Phi}(x) = \sum_{\alpha\in\mathbb{Z}^d} \widetilde{A}_\alpha\widetilde{\Phi}(Mx-\alpha), \quad \widetilde{\Psi}^\lambda(x) = \sum_{\alpha\in\mathbb{Z}^d} \widetilde{A}^\lambda_\alpha\widetilde{\Phi}(Mx-\alpha).$$

The following theorem is due to Dahmen [8].

Theorem 3.3. *Assume that $\mathbf{\Psi}$ and $\widetilde{\mathbf{\Psi}}$ are dual Riesz bases in $L_2(\mathbb{R}^d)$ with compactly supported basis functions. In particular the symbols $P(\omega)$ and $\widetilde{P}(\omega)$ of the scaling functions Φ resp. $\widetilde{\Phi}$ are trigonometric polynomials (i.e. they have finitely supported masks $(A_\alpha)_\alpha, (\widetilde{A}_\alpha)_\alpha$). Then the regularity exponents of Φ and $\widetilde{\Phi}$ are positive, and*

$$\begin{aligned} \mathbf{\Psi} \text{ is a Riesz basis in } H^s(\mathbb{R}^d) &\quad\Leftrightarrow\quad -s_{\widetilde{\Phi}} < s < s_\Phi, \\ \widetilde{\mathbf{\Psi}} \text{ is a Riesz basis in } H^s(\mathbb{R}^d) &\quad\Leftrightarrow\quad -s_\Phi < s < s_{\widetilde{\Phi}}. \end{aligned}$$

Theorem 3.3 is not always applicable because it assumes that $\widetilde{\Phi} \in L_2(\mathbb{R}^d)^{r\times 1}$, which can be checked by Theorem 3.1. Generally we do not know in advance whether our multilevel system $\mathbf{\Psi}$ of the form (13) is an L_2 Riesz basis. Therefore, it is possible that the dual system only exists in distributional sense in L_2 which is not sufficient. In that case we cannot use Theorem 3.2 either to compute $s_{\widetilde{\Phi}}$. This problem was solved by Lorentz and Oswald in [21] for the case $r = 1$. For the remainder of this section we will treat here the more general case $r \geq 1$ which is a straightforward generalization of the results in [21]. We prove the following theorem.

Theorem 3.4. *Assume that $\mathbf{\Psi}$ and $\widetilde{\mathbf{\Psi}}$ only contain compactly supported basis functions. If $\widetilde{s} := -\frac{d}{2}\log_m \widetilde{\rho} \leq 0$ satisfies $-\widetilde{s} < s_\Phi$ with $\widetilde{\rho} := \max\{|\nu| : \nu \in \operatorname{spec}(T_{\widetilde{P}}\big|_{\mathbb{H}})\}$, then the multilevel system $\mathbf{\Psi}$ of the form (13) is a Riesz basis in $H^s(\mathbb{R}^d)$ for all s in the interval*

$$-\widetilde{s} < s < s_\Phi.$$

Furthermore, $\mathbf{\Psi}$ is not a Riesz basis in $H^s(\mathbb{R}^d)$ for any $s < -\widetilde{s}$.

First we introduce some notation and we prove some auxiliary lemmas. Suppose that $(c_\alpha)_\alpha$ is a sequence of $r \times 1$ vectors, then we denote the periodic function vector

$$c(\omega) := \sum_{\alpha\in\mathbb{Z}^d} c_\alpha e^{-i\alpha\cdot\omega}$$

by the same letter. Likewise we have

$$c^T(\omega) := \sum_{\alpha\in\mathbb{Z}^d} c_\alpha^T e^{-i\alpha\cdot\omega}.$$

We introduce the matrix function

$$L(\omega) := \left(P^{\lambda_j}(\omega + 2\pi M^{-T}\lambda_i)\right)_{i,j\in\Lambda},$$

which is invertible for all $\omega \in \mathbb{T}$ if and only if $\{\Phi(x-\alpha), \Psi(x-\alpha), \alpha \in \mathbb{Z}^d\}$ is a L_2 Riesz basis in V_1, see [33, Theorem 13]. For our purposes this is satisfied, see Theorem 2.1. From (5) and (6) we get

$$L^{-1}(\omega) = \left(\widetilde{P}^{\lambda_i}(\omega + 2\pi M^{-T}\lambda_j)^*\right)_{i,j\in\Lambda}. \tag{16}$$

Lemma 3.5. *Consider the unique decomposition of $v_1 \in V_1$:*

$$v_1 := \sum_{\alpha\in\mathbb{Z}^d} c_\alpha^T \Phi(M\cdot - \alpha) = v_0 + w_1,$$

with

$$v_0 := \sum_{\beta\in\mathbb{Z}^d} (d_\beta^{\lambda_0})^T \Phi(\cdot - \beta) \in V_0, \qquad w_1 := \sum_{\lambda\in\Lambda'} \sum_{\beta\in\mathbb{Z}^d} (d_\beta^{\lambda})^T \Psi(\cdot - \beta) \in W_1.$$

Then

$$d^{\lambda_0}(M\omega) = m^{-1} \sum_{j=0}^{m-1} \widetilde{P}^{\lambda_j}(\omega + 2\pi M^{-T}\lambda_j)^* c(\omega + 2\pi M^{-T}\lambda_j). \tag{17}$$

Proof. This is a straightforward generalization of Eq. (41) in [21]. □

Let us define the projection operators

$$Q_j f := \sum_{\alpha\in\mathbb{Z}^d} \langle \widetilde{\Phi}(M^j \cdot - \alpha), f\rangle_{L_2} \Phi(M^j \cdot - \alpha).$$

These operators satisfy $Q_j Q_{j+k} = Q_j$ for all $0 \leq j, k < \infty$. We also define the following norm on $C_0(\mathbb{T})^{r\times r}$:

$$\|T_P^k H\|_\infty := \sum_{1\leq i,j\leq r} \sup_{\omega\in\mathbb{T}}\{|e_i^T T_P^k H(\omega) e_j|\},$$

with e_i, e_j the i-th resp. j-th column of I_r, and

$$\| T_P^k\big|_{\mathbb{H}} \|_\infty := \sup_{H\in\mathbb{H}} \frac{\|T_P^k H\|_\infty}{\|H\|_\infty}.$$

Lemma 3.6. *For arbitrary $k>0$ we have the norm equivalence*

$$\| Q_j\big|_{V_{j+k}} \|_{L_2}^2 = \| Q_0\big|_{V_k} \|_{L_2}^2 \sim \|T_{\widetilde{P}}^k I_r\|_\infty.$$

Proof. First we show that $\| Q_0|_{V_1} \|_{L_2}^2 \sim \|T_{\widetilde{P}} I_r\|_\infty$. Define v_0, v_1 and w_1 as in Lemma 3.5. Then, by the Riesz basis property of $\{\Phi(M^j\cdot -\alpha), \alpha\in\mathbb{Z}^d\}$ and because $\{e^{i\alpha\cdot\omega}, \alpha\in\mathbb{Z}^d, \omega\in\mathbb{T}\}$ is an orthonormal basis for $L_2(\mathbb{T})$,

$$\| Q_0\big|_{V_1} \|_{L_2}^2 = \sup_{v_1\neq 0}\frac{\|Q_0 v_1\|_{L_2}^2}{\|v_1\|_{L_2}^2} \sim m\sup_{c\neq 0}\frac{\|d^{\lambda_0}\|_{F(\mathbb{T})}^2}{\|c\|_{F(\mathbb{T})}^2},$$

where

$$\|d\|_{F(\mathbb{T})}^2 := \sum_{1\le j\le r} \|d_j\|_{L_2(\mathbb{T})}^2$$

is the Frobenius norm of the function vector $d(\omega) = [d_1(\omega)\cdots d_r(\omega)]^T$. Note that we have the equivalence

$$\max_j \|d_j\|_{L_2(\mathbb{T})}^2 \le \|d\|_{F(\mathbb{T})}^2 \le r\max_j \|d_j\|_{L_2(\mathbb{T})}^2. \tag{18}$$

Now we use Lemma 3.5, eq. (18), and Hölder's inequality to derive that

$$\begin{aligned}
m\|d\|_{F(\mathbb{T})}^2 &= m^2\|d(M\cdot)\|_{F(M^{-T}\mathbb{T})}^2 = \|\sum_{k=0}^{m-1}\widetilde{P}(\omega+2\pi M^{-T}\lambda_k)^* c(\omega+2\pi M^{-T}\lambda_k)\|_{F(M^{-T}\mathbb{T})}^2\\
&\sim \max_j \int_{M^{-T}\mathbb{T}} \left|\sum_{k=0}^{m-1}\sum_{i=1}^{r}\widetilde{P}_{ij}\overline{(\omega+2\pi M^{-T}\lambda_k)}c_i(\omega+2\pi M^{-T}\lambda_k)\right|^2 d\omega\\
&\le \max_j \int_{M^{-T}\mathbb{T}} \left(\sum_{k=0}^{m-1}\sum_{i=1}^{r}|\widetilde{P}_{ij}(\omega+2\pi M^{-T}\lambda_k)|^2\right)\left(\sum_{k=0}^{m-1}\|c(\omega+2\pi M^{-T}\lambda_k)\|_{l_2}^2\right)d\omega\\
&\le \sum_{i,j=1}^{r}\left\|\sum_{k=0}^{m-1}\widetilde{P}_{ij}(\omega+2\pi M^{-T}\lambda_k)\widetilde{P}_{ij}\overline{(\omega+2\pi M^{-T}\lambda_k)}\right\|_{L_\infty(M^{-T}\mathbb{T})}\\
&\quad\cdot\int_{M^{-T}\mathbb{T}}\left(\sum_{k=0}^{m-1}\|c(\omega+2\pi M^{-T}\lambda_k)\|_{l_2}^2\right)d\omega\\
&= \|T_{\widetilde{P}} I_r\|_\infty\cdot\|c\|_{F(\mathbb{T})}^2.
\end{aligned}$$

Thus we have $\| Q_0|_{V_1} \|_{L_2}^2 \lesssim \|T_{\widetilde{P}} I_r\|_\infty$. Since Hölder's inequality is a sharp estimate we can find a function vector $c(\omega)$ such that

$$m\|d\|_{F(\mathbb{T})}^2 \sim \max_j \int_{M^{-T}\mathbb{T}} \left(\sum_{k=0}^{m-1}\sum_{i=1}^{r}|\widetilde{P}_{ij}(\omega+2\pi M^{-T}\lambda_k)|^2\right)\left(\sum_{k=0}^{m-1}\|c(\omega+2\pi M^{-T}\lambda_k)\|_{l_2}^2\right)d\omega.$$

Indeed, take $c(\omega) = a(\omega)\left(\widetilde{P}_{ij}(\omega)\right)_{i=1}^{r}$ with $a(\omega)$ an arbitrary measurable function on $M^{-T}\mathbb{T}$. Now choose $a(\omega)$ as the characteristic function of the set of all $\omega\in M^{-T}\mathbb{T}$ for which for arbitrary i,j

$$\sum_{k=0}^{m-1}|\widetilde{P}_{ij}(\omega+2\pi M^{-T}\lambda_k)|^2 \ge (1-\epsilon)\left\|\sum_{k=0}^{m-1}|\widetilde{P}_{ij}(\omega+2\pi M^{-T}\lambda_k)|^2\right\|_{L_\infty(M^{-T}\mathbb{T})}$$

and let $\epsilon \to 0$. We find

$$\begin{aligned} m\|d\|^2_{F(\mathbb{T})} &\sim \max_j \sum_{i=1}^r \left\| \sum_{k=0}^{m-1} |\widetilde{P}_{ij}(\omega + 2\pi M^{-T}\lambda_k)|^2 \right\|_{L_\infty(M^{-T}\mathbb{T})} \\ &\quad \cdot \int_{M^{-T}\mathbb{T}} \left(\sum_{k=0}^{m-1} \|c(\omega + 2\pi M^{-T}\lambda_k)\|^2_{l_2} \right) d\omega \\ &\sim \|T_{\widetilde{P}} I_r\|_\infty \cdot \|c\|^2_{F(\mathbb{T})}. \end{aligned}$$

Hence $\| Q_0|_{V_1} \|^2_{L_2} \sim \|T_{\widetilde{P}} I_r\|_\infty$. By iterating Lemma 3.5 one obtains $\| Q_0|_{V_k} \|^2_{L_2} \sim \|T^k_{\widetilde{P}} I_r\|_\infty$ in the same way. This concludes the proof. □

Proof of Theorem 3.4. It follows from properties of the spectral radius and Lemma 3.6 that

$$\|Q_j v_{j+k}\|^2_{L_2} \lesssim \sigma^{-2\widetilde{s}k} \|v_{j+k}\|^2_{L_2}, \qquad j,k \in \mathbb{N}, \quad v_{j+k} \in V_{j+k}. \tag{19}$$

Indeed, we have the equality $\widetilde{\rho} = \lim_{k\to\infty} \|(T_{\widetilde{P}}|_{\mathbb{H}})^k\|^{1/k}_\infty$. Choose an $\epsilon > 0$. The spectral radius of the operator $(\widetilde{\rho} + \epsilon)^{-1} T_{\widetilde{P}}|_{\mathbb{H}}$ is strictly smaller than one. Therefore we find that

$$\lim_{k\to\infty} \|((\widetilde{\rho} + \epsilon)^{-1} T_{\widetilde{P}}|_{\mathbb{H}})^k\|_\infty = 0,$$

such that for arbitrary $k > 0$ there exists a constant C_ϵ for which $\|((\widetilde{\rho} + \epsilon)^{-1} T_{\widetilde{P}}|_{\mathbb{H}})^k\|_\infty < C_\epsilon$, or

$$\|(T_{\widetilde{P}}|_{\mathbb{H}})^k\|_\infty \lesssim (\widetilde{\rho} + \epsilon)^k.$$

Because $I_r \in \mathbb{H}$ and $\|I_r\|_\infty \sim 1$ we find from Lemma 3.6 that

$$\|Q_j v_{j+k}\|^2_{L_2} \lesssim (\widetilde{\rho} + \epsilon)^k \|v_{j+k}\|^2_{L_2}.$$

By definition of $\widetilde{s}$ and by taking a sufficiently small $\epsilon > 0$ we find (19).

It is well known, see e.g. [27, Lemma 2], that

$$\|f\|^2_{H^s} \sim \inf_{v_j \in V_j : f = \sum_j v_j} \sum_{j=0}^\infty \sigma^{2js} \|v_j\|^2_{L_2} \tag{20}$$

for all $0 < s < s_\Phi$. Because of the norm equivalence (20) it is sufficient to show that

$$\inf_{v_j \in V_j : v_J = \sum_j v_j} \sum_{j=0}^J \sigma^{2js} \|v_j\|^2_{L_2)} \sim \sum_{j=0}^J \sigma^{2js} \|(Q_j - Q_{j-1}) v_J\|^2_{L_2}$$

for all $-\widetilde{s} < s < s_\Phi$ which follows from standard techniques as used in [26, 11, 23]. This equivalence implies the H^s Riesz basis property for the finite set

$$\mathbf{\Psi}_J := \{\Phi(x - \alpha), \sigma^{j(d/2-s)} \Psi^\lambda(M^j x - \alpha), \alpha \in \mathbb{Z}^d, j = 0, 1, \ldots, J,\ \lambda \in \Lambda'\}.$$

Then we let $J \to \infty$ to obtain the H^s Riesz basis property for the (normalized) multilevel system $\mathbf{\Psi}$.

Now suppose that $s < -\widetilde{s}$. Let $s' \in (s, -\widetilde{s})$. Similar to the derivation of eq. (19) we can now find a sequence $v_J \in V_J$ with $J \to \infty$ such that $\|Q_0 v_J\|^2_{L_2} \gtrsim \sigma^{2s'J} \|v_J\|^2_{L_2}$. Using (20) we obtain

$$\begin{aligned} \|v_J\|_{H^s} &\lesssim \inf_{v_j \in V_j : v_J = \sum_j v_j} \sum_{j=0}^J \sigma^{2js} \|v_j\|^2_{L_2} \lesssim \sigma^{2J(s-s')} \|Q_0 v_J\|^2_{L_2} \\ &\lesssim \sigma^{2J(s-s')} \left(\|Q_0 v_J\|^2_{L_2} + \sum_{j=1}^J \sigma^{2js} \|(Q_j - Q_{j-1}) v_J\|^2_{L_2} \right). \end{aligned}$$

The factor $\sigma^{2J(s-s')}$ goes exponentially fast to zero as $J \to \infty$. Therefore the equivalence

$$\|v_J\|_{H^s} \sim \sum_{j=0}^{J} \sigma^{2js} \|(Q_j - Q_{j-1})v_J\|_{L_2}^2$$

does not hold. This establishes Theorem 3.4.

□

Remark 3.7. Q. Jiang and P. Oswald have written Matlab routines for numerically estimating smoothness exponents, see their papers [17] and [18].

4 Examples and numerical experiments

4.1 Linear spline wavelets on $\mathbb{R}$

The shifts

$$\phi_{j,k} = \Phi(2^j - k), \qquad k \in \mathbb{Z},$$

of the generating function

$$\Phi(t) = \begin{cases} 1+t, & -1 \le t \le 0, \\ 1-t, & 0 \le t \le 1, \\ 0, & \text{else} \end{cases}$$

form a basis of the space of linear splines V_j with knots at $2^{-j}k$, $k \in \mathbb{Z}$. Furthermore the scaled set $\{2^{j/2}\phi_{j,k}, k \in \mathbb{Z}\}$ satisfies the Riesz basis property (4). The wavelets $\psi_{j,k}$ are initially defined as $\psi_{j,k} := \phi_{j+1,2k+1}$. It is easy to see that a scaling function $\phi_{j,k}$ corresponds to an old knot at $2^{-j}k$ while a wavelet function $\psi_{j,k}$ corresponds to a new knot at $2^{-j}k + 1/2$. We fix the update stencil in advance in order to have local support for the wavelet functions in W_j. A wavelet function $\psi_{j,k} \in W_j$ corresponding to a new knot $2^{-j}k + 1/2$ is updated by the two neighbouring scaling functions in V_j corresponding to the two neighbouring old knots $2^{-j}k$ and $2^{-j}(k+1)$. Applying the construction method described in Section 2 we find that

$$\psi_{j,k} = \phi_{j+1,2k+1} - \frac{1}{4}\phi_{j,k} - \frac{1}{4}\phi_{j,k+1}, \qquad k \in \mathbb{Z},$$

which is the CDF(2,2) wavelet [5]. The scaling functions and the duals satisfy the refinement relation

$$\begin{aligned} \Phi(t) &= \Phi(2t) + \frac{1}{2}\left(\Phi(2t-1) + \Phi(2t+1)\right), \qquad t \in \mathbb{R} \\ \widetilde{\Phi}(t) &= \frac{3}{2}\widetilde{\Phi}(2t) + \frac{1}{2}\left(\widetilde{\Phi}(2t-1) + \widetilde{\Phi}(2t+1)\right) - \frac{1}{4}\left(\widetilde{\Phi}(2t-2) + \widetilde{\Phi}(2t+2)\right), \quad t \in \mathbb{R}. \end{aligned}$$

It is well-known that $s_\Phi = 1.5$. So we only need to investigate the Sobolev regularity of the dual scaling function $\widetilde{\phi}$. Using Theorem 3.2 we compute in Matlab that $s_{\widetilde{\Phi}} \approx 0.440765$. From Theorem 3.3, the linear spline wavelets are a Riesz basis for $H^s(\mathbb{R})$ with $-0.440765 < s < 1.5$. Figure 1 depicts Φ, Ψ and $\widetilde{\Phi}$. Note that the wavelets have two vanishing moments, although our construction method only demands one vanishing moment.

Suppose that we do not demand a vanishing moment, but that we orthogonalize the wavelet $\psi_{j,k}$ to $\phi_{j,k}$ and $\phi_{j,k+1}$. Then we find that

$$\psi_{j,k} = \phi_{j+1,2k+1} - \frac{3}{10}\phi_{j,k} - \frac{3}{10}\phi_{j,k+1}, \qquad k \in \mathbb{Z},$$

which yields a Riesz basis for $H^s(\mathbb{R})$ with $0.064715 < s < 1.5$. As expected we do not get an L_2 stable Riesz basis.

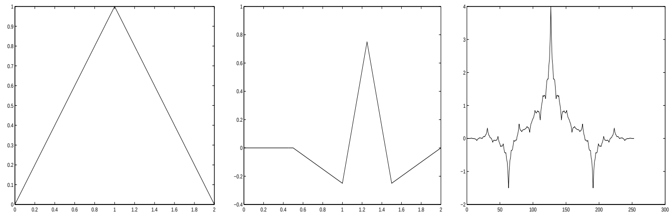

(a) Φ (b) Ψ (c) $\widetilde{\Phi}$

Figure 1: Linear spline wavelet on $\mathbb{R}$

In the introduction we motivated the use of wavelets for solving elliptic equations. Consider the two-point boundary value problem

$$-\frac{d^2u}{dx^2} + qu = f \quad \text{on} \quad \Omega := [0,2], \qquad u(0) = u(2) = 0.$$

If we take $f(x) = e^x(x^2(1-x)+2x(1+q)-2)$, then $u(x) = e^x x(2-x)$ is the exact solution. For the discretizations and solvers we use the linear finite element hierarchical basis and the linear wavelet basis constructed above. Near the boundary the wavelets are corrected following the strategy of Section 2 subjected to the boundary constraints. For instance, in the uniform setting we find that $\psi_{j,k} = \phi_{j+1,2k+1} - \frac{1}{2}\phi_{j,k}$ near the right boundary. To solve the boundary value problem we employ a nested iteration pcg-method with preconditioner the diagonal of the stiffness matrix. Tables 1 and 2 show the condition numbers κ of the related stiffness matrices for the cases $q = 1$ resp. $q = 10^8$. It is well known that for problems with q small wavelet basis methods perform slightly worse than traditional finite element preconditioners, as can be seen in Table 1. The situation changes when the value of q is increased. The better behaviour for the wavelet basis is due to its L_2-stability which becomes more important for large q.

	Linear wavelets			Linear FEM		
J	residual	#iter	κ	residual	#iter	κ
4	5.4698e-07	11	4.2707	2.0851e-07	4	1.2880
5	1.2344e-06	11	4.6169	7.7073e-07	3	1.2887
6	3.6515e-07	12	4.8821	1.9590e-07	3	1.2889
7	1.9800e-07	12	5.0910	4.9267e-08	3	1.2890
8	8.7367e-08	12	5.2576	1.2353e-08	3	1.2890
9	4.8193e-08	12	5.3925	5.8476e-08	2	1.2890
10	2.8160e-08	12	5.5031	1.4927e-08	2	1.2890
11	1.6413e-08	12	5.5949	3.7361e-09	2	1.2890
12	8.7869e-09	12	5.6717	9.3495e-10	2	1.2890

Table 1: Condition numbers, 1D problem, $q = 1$

4.2 Linear spline wavelets on $\mathbb{R}^2$

Let Δ by a type-1 triangulation, i.e. a triangulation formed by a rectangular partition plus north-east diagonals. Define the dilation matrix $M := 2I_2$. Each scaling function $\phi_{0,k}$ takes the value 1 at vertex $k \in \Delta$ and is zero at all other vertices. Let V_j be the space of linear splines with vertices at $M^{-j}\Delta$. We update a wavelet at a new vertex λ in $M^{-j-1}\Delta$ by the four old vertices $\gamma_1, \ldots, \gamma_4$ in $M^{-j}\Delta$ that define the two triangles $T(\gamma_1, \gamma_2, \gamma_3)$ and $T(\gamma_1, \gamma_2, \gamma_4)$ in $M^{-j}\Delta$ with common edge

	Linear wavelets			Linear FEM		
J	residual	#iter	κ	residual	#iter	κ
4	1.1129e-06	8	6.1018	5.7951e-07	14	120.9161
5	6.7558e-07	7	6.6487	9.5062e-07	16	287.7855
6	4.8828e-07	5	7.1602	6.1601e-07	16	667.1219
7	2.5155e-07	4	7.5836	2.4519e-07	15	1.5158e+03
8	1.3805e-07	2	7.9610	1.4319e-07	10	3.3852e+03
9	6.8250e-08	2	8.2814	7.4576e-08	11	7.4039e+03
10	2.2979e-08	2	8.5351	3.7296e-08	7	1.5504e+04
11	1.0952e-08	2	8.6829	1.8695e-08	12	2.8954e+04
12	4.4593e-09	1	8.7174	8.7550e-09	32	4.3179e+04

Table 2: Condition numbers, 1D problem, $q = 10^8$

$[\gamma_1, \gamma_2]$ containing λ. We find that

$$\psi_{j,\lambda} = \phi_{j+1,\lambda} - \frac{13}{80}\left(\phi_{j,\gamma_1} + \phi_{j,\gamma_2}\right) + \frac{3}{80}\left(\phi_{j,\gamma_3} + \phi_{j,\gamma_4}\right).$$

The scaling functions and the dual scaling functions satisfy

$$\begin{aligned}
\Phi(x) &= \Phi(Mx) + \frac{1}{2}\sum_{k\in K_1}\Phi(Mx-k), \qquad x\in\mathbb{R}^2,\\
\widetilde{\Phi}(x) &= \frac{41}{20}\widetilde{\Phi}(Mx) + \frac{13}{20}\sum_{k\in K_1}\widetilde{\Phi}(Mx-k) - \frac{7}{40}\sum_{k\in K_2}\widetilde{\Phi}(Mx-k)\\
&\quad -\frac{3}{20}\sum_{k\in K_3}\widetilde{\Phi}(Mx-k),\ x\in\mathbb{R}^2,
\end{aligned}$$

with

$$\begin{aligned}
K_1 &:= \{(0,1),(1,0),(-1,0),(0,-1),(1,-1),(-1,1)\},\\
K_2 &:= \{(0,2),(2,0),(-2,0),(0,-2),(2,-2),(-2,2)\},\\
K_3 &:= \{(1,1),(-1,-1),(-1,2),(-2,1),(1,-2),(2,-1)\}.
\end{aligned}$$

We find that $s_\Phi = 1.5$ and $s_{\widetilde{\Phi}} \approx 0.328857$ using Theorem 3.2. The bivariate linear spline wavelets are a Riesz basis for $H^s(\mathbb{R}^2)$ with $-0.328857 < s < 1.5$, and in the uniform setting they have two vanishing moments. Figure 2 depicts Φ, Ψ and $\widetilde{\Phi}$.

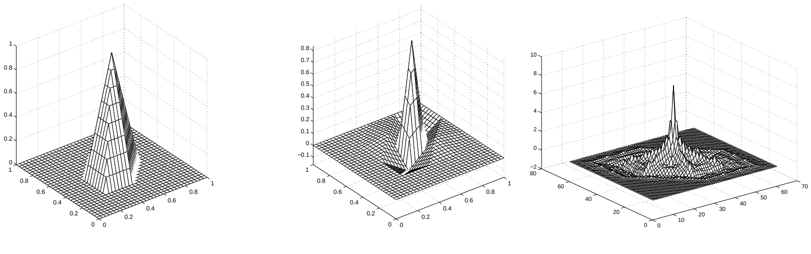

(a) Φ (b) Ψ (c) $\widetilde{\Phi}$

Figure 2: Linear spline wavelet on $\mathbb{R}^2$

Consider the elliptic problem

$$-\Delta u + qu = f \quad \text{on} \quad \Omega := [0,1]^2, \qquad u|_{\partial\Omega} = 0,$$

with $f(x,y) = 2y(1-y) + 2x(1-x) + qx(1-x)y(1-y)$. Then $u(x,y) = x(1-x)y(1-y)$ is the exact solution. For the discretizations and solvers we use the linear finite element hierarchical basis of Yserentant [38] which is suboptimal, and the above constructed bivariate linear spline wavelet basis. Near the boundary we correct the wavelets such that they satisfy the boundary conditions. They still have at least one vanishing moment and are as orthogonal as possible with respect to the scaling functions in the update stencil. To solve the elliptic problem we employ a nested iteration pcg-method with preconditioner the diagonal of the stiffness matrix. Tables 3 and 4 show the condition numbers κ of the related stiffness matrices for the cases $q = 1$ resp. $q = 10^8$.

	Linear wavelets			Linear FEM		
J	residual	#iter	κ	residual	#iter	κ
2	7.8652e-06	14	9.5693	1.1472e-05	14	10.6547
3	6.2326e-06	17	12.6641	6.7046e-06	18	19.6424
4	2.4594e-06	19	14.8823	2.7490e-06	21	32.0355
5	1.3077e-06	20	16.5042	1.3594e-06	25	47.4134
6	8.0308e-07	20	17.7386	9.8639e-07	28	65.7367

Table 3: Condition numbers, 2D problem, $q = 1$

	Linear wavelets			Linear FEM		
J	residual	#iter	κ	residual	#iter	κ
2	1.2125e-05	15	14.6164	1.3079e-05	16	108.2440
3	7.1122e-06	18	19.3987	5.8689e-06	35	607.5954
4	3.9788e-06	19	23.8976	3.9705e-06	58	3.1318e+03
5	1.9740e-06	20	27.7369	1.3060e-06	75	1.5344e+04
6	6.8437e-07	21	31.0350	9.0148e-07	92	7.2542e+04

Table 4: Condition numbers, 2D problem, $q = 10^8$

4.3 Quadratic spline wavelets on $\mathbb{R}^2$

Define the hexagonal lattice Δ in $\mathbb{R}^2$ as the image of $\mathbb{Z}^2$ under

$$\Gamma := \begin{bmatrix} 1 & -1/2 \\ 0 & \sqrt{3}/2 \end{bmatrix}, \tag{21}$$

and let Δ^* be its refinement by drawing in the additional grid lines $y = l$, $y = \frac{\sqrt{3}}{3}(x+m)$, and $y = -\frac{\sqrt{3}}{3}(x+n)$, $l,m,n \in \mathbb{Z}$. In fact, Δ^* is the Powell–Sabin 6-split of Δ, cfr. [29]. Define $S_2^1(\Delta^*)$ as the space of real-valued functions in $C^1(\mathbb{R}^2)$ whose restrictions on each triangle of the triangulation Δ^* are bivariate quadratic polynomials. Then each function $\phi \in S_2^1(\Delta^*)$ is called a Powell–Sabin (PS) spline. Let $k \in \Delta$, then the interpolation problem

$$\left[\phi(l), \frac{\partial}{\partial x}\phi(l), \frac{\partial}{\partial y}\phi(l)\right] = \delta_{k,l}\left[\alpha, \beta, \gamma\right], \qquad l \in \Delta, \tag{22}$$

has a unique solution $\phi \in S_2^1(\Delta^*)$, see [29]. This allows to define a function vector $\Phi = [\phi_1, \phi_2, \phi_3]^T$ that generates a multiresolution analysis (MRA). Let each ϕ_i, $i = 1,2,3$, be the unique solution of (22) with

$$\alpha = \frac{1}{3},\ \beta = \frac{8\sqrt{3}}{9} - \delta_{i,1}\frac{24\sqrt{3}}{9},\ \gamma = \left((-1)^{i-1} - \delta_{i,1}\right)\frac{8}{3},$$

then the integer translates under Γ of the basis functions ϕ_i form a basis for $S_2^1(\Delta^*)$, see [12]. Define the 2×2 dilation matrix $M := 3I_2$, then we consider the refinement $\Delta_j := M^{-j}\Delta$, and the corresponding PS 6-split $\Delta_j^* := M^{-j}\Delta^*$. We use a triadic refinement because this refinement is generally applicable to arbitary triangulations and their PS-refinements, while dyadic refinement may give artifacts in the PS-refinements [37]. In general, the basis function vectors on all standard refinements Δ_j of Δ can be written as

$$\phi_{j,k}(x) = \Phi(M^j x - \Gamma k), \qquad k \in \mathbb{Z}^2, \quad x \in \mathbb{R}^2,$$

and the set $\left\{3^j \phi_{j,k} \mid k \in \Delta_j\right\}$ forms an L^2-stable basis of V_j, see [24, 25]. The scaling vector Φ satisfies a matrix refinement equation of the form

$$\Phi(x) = \sum_{k \in \mathbb{Z}^2} A_k \Phi(Mx - \Gamma k), \quad x \in \mathbb{R}^2,$$

where the 3×3 mask coefficient matrices A_k are given in the Appendix. The update stencil for the wavelet function vectors is different for a new vertex on the edge or a new vertex in the interior of an old triangle. Both stencils are shown in Figure 3. A wavelet function of a new vertex on an edge is updated by the scaling function vectors of the two neighbouring old vertices on that edge. Because there are three basis functions associated with each function vector, the width of this stencil is six. For the wavelet functions of a new vertex in the interior of an old triangle, the scaling function vectors on the corners of the triangle are used. This yields a stencil of width nine. We refer to the paper [36] for a more detailed description. After an extensive but straightforward

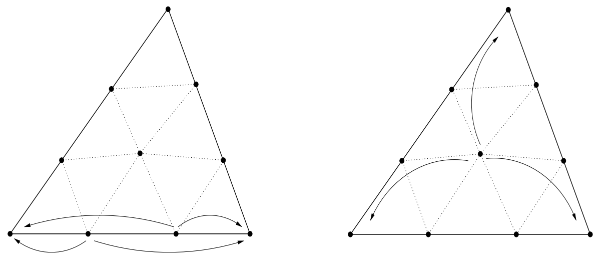

(a) vertex on edge (b) vertex in interior

Figure 3: The update stencil

computation we find that the dual scaling function vectors satisfy the refinement equation

$$\widetilde{\Phi}(x) = \sum_{k \in \mathbb{Z}^2} \widetilde{A}_k \widetilde{\Phi}(Mx - \Gamma k), \quad x \in \mathbb{R}^2,$$

where the 3×3 mask coefficient matrices $\widetilde{A}_k$ are given in the Appendix. These dual function vectors exist in L_2 in distributional sense (the symbol $\widetilde{P}(\omega)$ satisfies Condition E), but Theorem 3.1 is not satisfied. The transition operator $T_{\widetilde{P}}$ does not satisfy Condition E. Hence we cannot use Theorem 3.2 to estimate the range of stability, but we use Theorem 3.4 and we find that these Powell–Sabin spline wavelets are a Riesz basis for $H^s(\mathbb{R}^2)$ for all $0.802774 < s < 2.5$. Figure 4 depicts Φ and Ψ.

5 Customizing wavelets on uniform grids

When working on uniform grids all computations can be done in advance. The lifting scheme allows us to create wavelets with certain properties such as vanishing moments, symmetry, etc. The remaining degrees of freedom can be chosen in such a way that the range of stability is as large as possible by solving a minimization problem. Let us demonstrate this principle with an

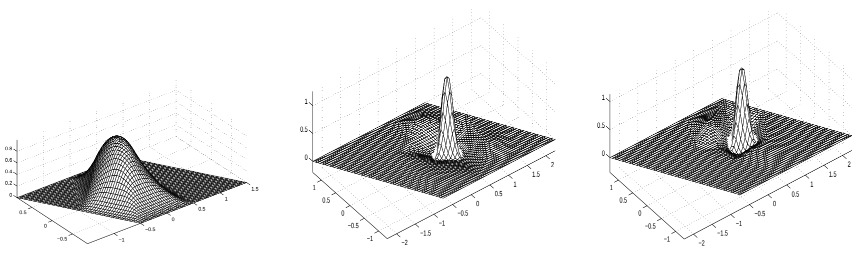

(a) Φ (b) Ψ (interior vertex) (c) Ψ (vertex on edge)

Figure 4: Quadratic spline wavelet on $\mathbb{R}^2$

example. Consider the piecewise Hermite cubics defined by

$$\begin{aligned}\phi_1(x) &:= \begin{cases} (x+1)^2(-2x+1), & x \in [-1,0], \\ (1-x)^2(2x+1), & x \in [0,1] \end{cases} \\ \phi_2(x) &:= \begin{cases} (x+1)^2 x, & x \in [-1,0], \\ (1-x)^2 x, & x \in [0,1] \end{cases} .\end{aligned}$$

Integer translates of ϕ_1, ϕ_2 generate the space of C^1 piecewise cubic functions on $\mathbb{R}$ which interpolate function values and first derivatives at the integers. Define the generator $\Phi(x) = (\phi_1(x), \phi_2(x))^T$. Then $\Phi(x)$ satisfies the refinement equation

$$\Phi(x) = \begin{bmatrix} \frac{1}{2} & \frac{3}{4} \\ -\frac{1}{8} & -\frac{1}{8} \end{bmatrix} \Phi(2x+1) + \begin{bmatrix} 1 & 0 \\ 0 & \frac{1}{2} \end{bmatrix} \Phi(2x) \begin{bmatrix} \frac{1}{2} & -\frac{3}{4} \\ \frac{1}{8} & -\frac{1}{8} \end{bmatrix} \Phi(2x-1).$$

The wavelets can be represented by the generator $\Psi(x) = (\psi_1(x), \psi_2(x))^T$. We define the update stencil for a new grid point as the two neighbouring coarser grid points. So we get

$$\Psi(x) = \Phi(2x-1) - \begin{bmatrix} \alpha_1 & \alpha_2 \\ \beta_1 & \beta_2 \end{bmatrix} \Phi(x) - \begin{bmatrix} \alpha_3 & \alpha_4 \\ \beta_3 & \beta_4 \end{bmatrix} \Phi(x-1).$$

Suppose that we want two vanishing moments, ψ_1 has to be symmetric and ψ_2 has to be anti-symmetric. Then we need 6 degrees of freedom to satisfy these properties. Hence 2 degrees of freedom remain and the dual generator $\widetilde{\Phi}(x)$ satisfies the refinement equation

$$\begin{aligned}\widetilde{\Phi}(x) \quad = \quad & \begin{bmatrix} -\frac{9}{40} - \frac{\beta_2}{5} & -\frac{7}{60} - \frac{\beta_2}{15} \\ \alpha_2 + \frac{3\beta_2}{2} & \frac{\alpha_2+\beta_2}{2} \end{bmatrix} \widetilde{\Phi}(2x+2) + \begin{bmatrix} \frac{1}{2} & \frac{1}{30} - \frac{4\beta_2}{15} \\ -2\alpha_2 & 2\beta_2 \end{bmatrix} \widetilde{\Phi}(2x+1) \\ & + \begin{bmatrix} \frac{29}{20} + \frac{2\beta_2}{5} & 0 \\ 0 & 4 - \alpha_2 + \beta_2 \end{bmatrix} \widetilde{\Phi}(2x) \\ & + \begin{bmatrix} \frac{1}{2} & -\frac{1}{30} + \frac{4\beta_2}{15} \\ 2\alpha_2 & 2\beta_2 \end{bmatrix} \widetilde{\Phi}(2x-1) + \begin{bmatrix} -\frac{9}{40} - \frac{\beta_2}{5} & \frac{7}{60} + \frac{\beta_2}{15} \\ -\alpha_2 - \frac{3\beta_2}{2} & \frac{\alpha_2+\beta_2}{2} \end{bmatrix} \widetilde{\Phi}(2x-2)\end{aligned}$$

Theorems 3.3 and 3.4 characterize the range of stability, and Theorem 3.2 tells us how to compute the smoothness of $\widetilde{\Phi}(x)$. We use the minimization toolbox in Matlab to compute the optimal values (i.e. those values that give the largest range of stability) for the two remaining degrees of freedom α_2 and β_2 . We find $\alpha_2 = \frac{11}{7}$ and $\beta_2 = -\frac{6}{11}$, or

$$\Psi(x) = \Phi(2x-1) - \begin{bmatrix} \frac{1}{4} & \frac{11}{7} \\ -\frac{59}{660} & -\frac{6}{11} \end{bmatrix} \Phi(x) - \begin{bmatrix} \frac{1}{4} & -\frac{11}{7} \\ \frac{59}{660} & -\frac{6}{11} \end{bmatrix} \Phi(x-1).$$

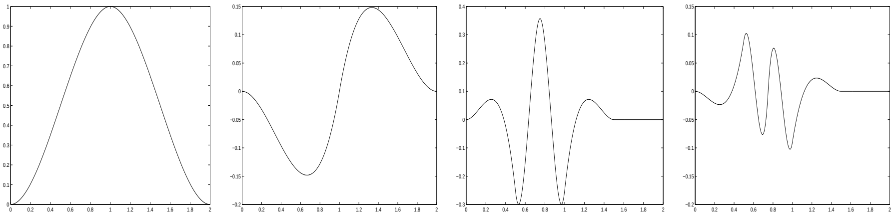

(a) ϕ_1 (b) ϕ_2 (c) ψ_1 (d) ψ_2

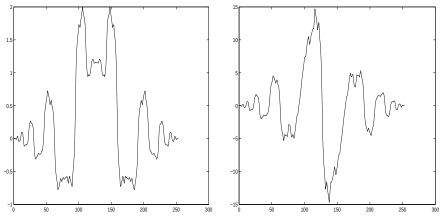

(e) $\widetilde{\phi}_1$ (f) $\widetilde{\phi}_2$

Figure 5: Cubic Hermite spline wavelet on $\mathbb{R}$

These wavelets are stable for $H^s(\mathbb{R})$ with $-0.828823 < s < 2.5$. Figure 5 visualizes the constructed functions. Note that these cubic Hermite spline wavelets are similar to the ones constructed in [9].

We conclude with a last example. Let us try to construct linear wavelets in $\mathbb{R}^2$ on the hexagonal lattice. We want them to have two vanishing moments, and we want hexagonal symmetry. If we use the same setting as in Section 4.2, then we initially have

$$\psi_{j,\lambda} = \phi_{j+1,\lambda} - \alpha_1 \phi_{j,\gamma_1} - \alpha_2 \phi_{j,\gamma_2} - \alpha_3 \phi_{j,\gamma_3} - \alpha_4 \phi_{j,\gamma_4}.$$

After some straightforward algebra we find that, in order to satisfy our wish list, we need three degrees of freedom out of four. Hence we keep one degree of freedom to stabilize our wavelet. The dual $\widetilde{\Phi}(x)$ satisfies

$$\begin{aligned}\widetilde{\Phi}(x) \quad &= \quad (4-12\alpha_1)\widetilde{\Phi}(Mx) + 4\alpha_1 \sum_{k\in K_1} \widetilde{\Phi}(Mx - \Gamma k) + (2\alpha_1 - \frac{1}{2}) \sum_{k \in K_2} \widetilde{\Phi}(Mx - \Gamma k) \\ &\quad + (\frac{1}{2} - 4\alpha_1) \sum_{k\in K_3} \widetilde{\Phi}(Mx - \Gamma k), \ x \in \mathbb{R}^2,\end{aligned}$$

with Γ as defined in (21). The optimal value for α_1 is computed with the optimization toolbox of Matlab and we find $\alpha_1 = \frac{3}{16}$. The resulting wavelet

$$\psi_{j,\lambda} = \phi_{j+1,\lambda} - \frac{3}{16}\left(\phi_{j,\gamma_1} + \phi_{j,\gamma_2}\right) + \frac{1}{16}\left(\phi_{j,\gamma_3} + \phi_{j,\gamma_4}\right)$$

is the same as the one constructed in [7] and the multilevel basis is a stable basis for $H^s(\mathbb{R}^2)$ with $-0.440765 < s < 1.5$.

Acknowledgements

This work is partially supported by the Flemish Fund for Scientific Research (FWO Vlaanderen) projects MISS (G.0211.02) and SMID (G.0431.05), and by the Belgian Programme on Interuniversity Attraction Poles, initiated by the Belgian Federal Science Policy Office. The scientific responsibility rests with the authors.

References

[1] R. A. Adams. *Sobolev spaces.* Academic Press, New York, 1975.

[2] J. M. Carnicer, W. Dahmen, and J. M. Peña. Local decomposition of refinable spaces. *Appl. Comp. Harm. Anal.*, 3:127–153, 1996.

[3] A. Cohen, W. Dahmen, and R. DeVore. Adaptive wavelet techniques in numerical simulation. *Encyclopedia of Computational Mathematics*, 1:157–197, 2004.

[4] A. Cohen and I. Daubechies. A new technique to estimate the regularity of refinable functions. *Rev. Mat. Iberoamericana*, 12(2):527–591, 1996.

[5] A. Cohen, I. Daubechies, and J.-C. Feauveau. Biorthogonal bases of compactly supported wavelets. *Comm. Pure Appl. Math.*, 45(5):485–560, 1992.

[6] A. Cohen and R. Masson. Wavelet methods for second-order elliptic problems, preconditioning, and adaptivity. *SIAM J. Sci. Comput.*, 21(3):1006–1026, 1999.

[7] A. Cohen and J.-M. Schlenker. Compactly supported bidimensional wavelet bases with hexagonal symmetry. *Constr. Approx.*, 9:209–236, 1993.

[8] W. Dahmen. Stability of multiscale transformations. *J. Fourier Anal. Appl.*, 4:341–362, 1996.

[9] W. Dahmen, B. Han, R.-Q. Jia, and A. Kunoth. Biorthogonal multiwavelets on the interval: Cubic hermite splines. *Constr. Approx.*, 16:221–259, 2000.

[10] W. Dahmen and A. Kunoth. Multilevel preconditioning. *Numer. Math.*, 63:315–344, 1992.

[11] W. Dahmen, P. Oswald, and X.-Q. Shi. C^1-hierarchical bases. *J. Comput. Appl. Math.*, 51:37–56, 1994.

[12] P. Dierckx. On calculating normalized Powell–Sabin B-splines. *Comput. Aided Geom. Design*, 15(3):61–78, 1997.

[13] B. Han and R.-Q. Jia. Multivariate refinement equations and convergence of subdivision schemes. *SIAM J. Math. Anal.*, 29:1177–1199, 1998.

[14] S. Jaffard. Wavelet methods for fast resolution of elliptic problems. *SIAM J. Numer. Anal.*, 29(4):965–986, 1992.

[15] R.-Q. Jia and Q. Jiang. Spectral analysis of the transition operator and its applications to smoothness analysis of wavelets. *SIAM J. of Matrix Anal. and Appl.*, 24:1071–1109, 2003.

[16] Q. Jiang. Multivariate matrix refinable functions with arbitrary matrix dilation. *Trans. Amer. Math. Soc.*, 351:2407–2438, 1999.

[17] Q. Jiang and P. Oswald. On the analysis of $\sqrt{3}$-subdivision schemes. Preprint, 2003.

[18] Q. Jiang and P. Oswald. Triangular $\sqrt{3}$-subdivision schemes: the regular case. *J. Comput. Appl. Math*, 156:47–75, 2003.

[19] J. Ko, A. J. Kurdila, and P. Oswald. Scaling function and wavelet preconditioners for second order elliptic problems. In W. Dahmen, A. J. Kurdila, and P. Oswald, editors, *Multiscale Wavelet Methods for Partial Differential Equations*, volume 6, pages 413–438. Academic Press, San Diego, 1997.

[20] W. Lawton, S. L. Lee, and Z. Shen. Convergence of multidimensional cascade algorithms. *Numer. Math.*, 78:427–438, 1998.

[21] R. Lorentz and P. Oswald. Criteria for hierarchical bases in Sobolev spaces. *Appl. Comput. Harm. Anal.*, 8:32–85, 2000.

[22] M. Lounsbery, T. D. DeRose, and J. Warren. Multiresolution analysis for surfaces of arbitrary topological type. *ACM Trans. on Graphics*, 16(1):34–73, 1997.

[23] J. Maes and A. Bultheel. C^1 Hierarchical Riesz bases of Lagrange type on Powell–Sabin triangulations. *J. Comput. Appl. Math.* In press.

[24] J. Maes and A. Bultheel. Stable multiresolution analysis on triangles for surface compression. 2005. Submitted.

[25] J. Maes, E. Vanraes, P. Dierckx, and A. Bultheel. On the stability of normalized Powell–Sabin B-splines. *J. Comput. Appl. Math.*, 170(1):181–196, 2004.

[26] P. Oswald. Hierarchical conforming finite element methods for the biharmonic equation. *SIAM J. Numer. Anal.*, 29:1610–1625, 1992.

[27] P. Oswald. Multilevel solvers for elliptic boundary value problems on domains. In W. Dahmen, A. J. Kurdila, and P. Oswald, editors, *Multiscale Wavelet Methods for Partial Differential Equations*, volume 6, pages 3–58. Academic Press, San Diego, 1997.

[28] G. Plonka and V. Strela. From wavelets to multiwavelets. In *Mathematical Methods for Curves and Surfaces II.* Vanderbilt University Press, Nashville, TN, 1998.

[29] M. J. D. Powell and M. A. Sabin. Piecewise quadratic approximations on triangles. *ACM Trans. on Math. Software*, 3:316–325, 1977.

[30] A. Ron and Z. Shen. The sobolev regularity of refinable functions. *J. Approx. Theory*, 106:185–225, 2000.

[31] Z. Shen. Refinable function vectors. *SIAM J. Math. Anal.*, 29:235–250, 1998.

[32] J. Simoens and S. Vandewalle. A stabilized lifting construction of wavelets on irregular meshes on the interval. *SIAM J. Sci. Comput.*, 24(4):1356–1378, 2002.

[33] J. Stöckler. Multivariate wavelets. In C. K. Chui, editor, *Wavelets: A Tutorial in Theory and Applications*, pages 325–355. Academic Press, Boston, 1992.

[34] W. Sweldens. The lifting scheme: A custom-design construction of biorthogonal wavelets. *Appl. Comput. Harmon. Anal.*, 3(2):186–200, 1996.

[35] W. Sweldens. The lifting scheme: A construction of second generation wavelets. *SIAM J. Math. Anal.*, 29(2):511–546, 1997.

[36] E. Vanraes, J. Maes, and A. Bultheel. Powell–Sabin spline wavelets. *Intl. Journal of Wavelets, Multiresolution and Information Processing*, 2(1):23–42, 2004.

[37] E. Vanraes, J. Windmolders, A. Bultheel, and P. Dierckx. Automatic construction of control triangles for subdivided Powell–Sabin splines. *Comput. Aided Geom. Design*, 21(7):671–682, 2004.

[38] H. Yserentant. On the multi-level splitting of finite element spaces. *Numer. Math.*, 49:379–412, 1986.

Appendix

$$A_{(-2,-2)} = \frac{1}{9}\begin{bmatrix} 1 & 0 & 2 \\ 0 & 1 & 2 \\ 0 & 0 & 0 \end{bmatrix} \quad A_{(-1,-2)} = \frac{1}{9}\begin{bmatrix} 1 & 0 & 2 \\ 2 & 0 & 4 \\ 0 & 0 & 0 \end{bmatrix} \quad A_{(0,-2)} = \frac{1}{9}\begin{bmatrix} 1 & 0 & 0 \\ 2 & 0 & 2 \\ 0 & 0 & 1 \end{bmatrix}$$

$$A_{(-2,-1)} = \frac{1}{9}\begin{bmatrix} 0 & 2 & 4 \\ 0 & 1 & 2 \\ 0 & 0 & 0 \end{bmatrix} \quad A_{(-1,-1)} = \frac{1}{9}\begin{bmatrix} 4 & 2 & 4 \\ 2 & 4 & 4 \\ 0 & 0 & 1 \end{bmatrix} \quad A_{(0,-1)} = \frac{1}{27}\begin{bmatrix} 8 & 2 & 2 \\ 14 & 11 & 14 \\ 2 & 2 & 8 \end{bmatrix}$$

$$A_{(1,-1)} = \frac{1}{9}\begin{bmatrix} 0 & 0 & 0 \\ 4 & 0 & 2 \\ 2 & 0 & 1 \end{bmatrix} \quad A_{(-2,0)} = \frac{1}{9}\begin{bmatrix} 0 & 2 & 2 \\ 0 & 1 & 0 \\ 0 & 0 & 1 \end{bmatrix} \quad A_{(-1,0)} = \frac{1}{27}\begin{bmatrix} 11 & 14 & 11 \\ 2 & 8 & 2 \\ 2 & 2 & 8 \end{bmatrix}$$

$$A_{(0,0)} = \frac{1}{9}\begin{bmatrix} 5 & 2 & 2 \\ 2 & 5 & 2 \\ 2 & 2 & 5 \end{bmatrix} \quad A_{(1,0)} = \frac{1}{9}\begin{bmatrix} 1 & 0 & 0 \\ 4 & 4 & 2 \\ 4 & 2 & 4 \end{bmatrix} \quad A_{(2,0)} = \frac{1}{9}\begin{bmatrix} 0 & 0 & 0 \\ 2 & 1 & 0 \\ 2 & 0 & 1 \end{bmatrix}$$

$$A_{(-1,1)} = \frac{1}{9}\begin{bmatrix} 0 & 4 & 2 \\ 0 & 0 & 0 \\ 0 & 2 & 1 \end{bmatrix} \quad A_{(0,1)} = \frac{1}{9}\begin{bmatrix} 4 & 4 & 2 \\ 0 & 1 & 0 \\ 2 & 4 & 4 \end{bmatrix} \quad A_{(1,1)} = \frac{1}{27}\begin{bmatrix} 8 & 2 & 2 \\ 2 & 8 & 2 \\ 14 & 14 & 11 \end{bmatrix}$$

$$A_{(2,1)} = \frac{1}{9}\begin{bmatrix} 0 & 0 & 0 \\ 2 & 1 & 0 \\ 4 & 2 & 0 \end{bmatrix} \quad A_{(0,2)} = \frac{1}{9}\begin{bmatrix} 1 & 2 & 0 \\ 0 & 0 & 0 \\ 0 & 2 & 1 \end{bmatrix} \quad A_{(1,2)} = \frac{1}{9}\begin{bmatrix} 1 & 2 & 0 \\ 0 & 0 & 0 \\ 2 & 4 & 0 \end{bmatrix}$$

$$A_{(2,2)} = \frac{1}{9}\begin{bmatrix} 1 & 0 & 0 \\ 0 & 1 & 0 \\ 2 & 2 & 0 \end{bmatrix}$$

$$\widetilde{A}_{(0,-3)} = \begin{bmatrix} -2.649638565381197e-02 & -2.514504381498399e-01 & 9.514997716772432e-02 \\ -5.581998732161597e-02 & 1.999268785252507e-01 & 2.180269911861705e-03 \\ 9.760360498942661e-02 & -1.146852652986162e-01 & -6.314130668832016e-02 \end{bmatrix}$$

$$\widetilde{A}_{(3,-3)} = \begin{bmatrix} 3.329551186394467e-02 & 1.423407357673028e-01 & -7.066116934061388e-02 \\ 8.901291608157143e-02 & -8.433313451435348e-02 & -2.278582915002053e-03 \\ -2.154174283048086e-01 & -1.700183099895091e-01 & 1.613268088335274e-01 \end{bmatrix}$$

$$\widetilde{A}_{(0,-2)} = \begin{bmatrix} -1.027319934536386e-03 & 2.627238299781715e-02 & -2.058238042526939e-02 \\ 6.193084283933032e-04 & -4.141873962772590e-02 & 6.193084283933032e-04 \\ -2.058238042526939e-02 & 2.627238299781715e-02 & -1.027319934536386e-03 \end{bmatrix}$$

$$\widetilde{A}_{(1,-2)} = \begin{bmatrix} 5.793682782654931e-03 & 2.507253131582465e-02 & 6.170822938557453e-03 \\ -4.879655861320484e-02 & -8.732934266712920e-02 & -2.009176890381660e-02 \\ 8.003991286758694e-02 & 1.276464109542424e-01 & 2.260542043639538e-02 \end{bmatrix}$$

$$\widetilde{A}_{(2,-2)} = \begin{bmatrix} -3.855405958898559e-03 & -2.341046644963156e-02 & 2.033351440574390e-03 \\ -2.341046644963156e-02 & -3.855405958898559e-03 & 2.033351440574390e-03 \\ 2.768642600999824e-02 & 2.768642600999824e-02 & -3.576256757900155e-02 \end{bmatrix}$$

$$\widetilde{A}_{(-1,-1)} = \begin{bmatrix} 2.260542043639538e-02 & 8.003991286758694e-02 & 1.276464109542424e-01 \\ 6.170822938557453e-03 & 5.793682782654931e-03 & 2.507253131582465e-02 \\ -2.009176890381660e-02 & -4.879655861320484e-02 & -8.732934266712920e-02 \end{bmatrix}$$

$$\widetilde{A}_{(0,-1)} = \begin{bmatrix} 1.661307926654759e-01 & 1.541765874068727e-01 & 1.004418790233459e-01 \\ -1.558821141791788e-01 & -1.655461990047816e-01 & -1.558821141791788e-01 \\ 1.004418790233459e-01 & 1.541765874068727e-01 & 1.661307926654759e-01 \end{bmatrix}$$

$$\widetilde{A}_{(1,-1)} = \begin{bmatrix} -2.630104470330473e-02 & -9.198995834543475e-02 & -5.966619549478847e-02 \\ -9.198995834543475e-02 & -2.630104470330473e-02 & -5.966619549478847e-02 \\ 2.503925060912631e-01 & 2.503925060912631e-01 & 2.193174757327797e-01 \end{bmatrix}$$

$$\widetilde{A}_{(2,-1)} = \begin{bmatrix} -8.732934266712920e-02 & -2.009176890381660e-02 & -4.879655861320484e-02 \\ 1.276464109542424e-01 & 2.260542043639538e-02 & 8.003991286758694e-02 \\ 2.507253131582465e-02 & 6.170822938557453e-03 & 5.793682782654931e-03 \end{bmatrix}$$

$$\widetilde{A}_{(-3,0)} = \begin{bmatrix} 1.810136659133592e-01 & -2.252608568447245e-01 & -2.093920241491727e-01 \\ -2.553721632876749e-02 & 1.073353535802148e-02 & 5.209282974361006e-02 \\ -8.599110138394746e-02 & 1.308691753160441e-01 & 8.309190242353731e-02 \end{bmatrix}$$

$$\widetilde{A}_{(-2,0)} = \begin{bmatrix} -3.576256757900155e-02 & 2.768642600999824e-02 & 2.768642600999824e-02 \\ 2.033351440574390e-03 & -3.855405958898559e-03 & -2.341046644963156e-02 \\ 2.033351440574390e-03 & -2.341046644963156e-02 & -3.855405958898559e-03 \end{bmatrix}$$

$$\widetilde{A}_{(-1,0)} = \begin{bmatrix} 2.193174757327797e-01 & 2.503925060912631e-01 & 2.503925060912631e-01 \\ -5.966619549478847e-02 & -2.630104470330473e-02 & -9.198995834543475e-02 \\ -5.966619549478847e-02 & -9.198995834543475e-02 & -2.630104470330473e-02 \end{bmatrix}$$

$$\widetilde{A}_{(0,0)} = \begin{bmatrix} 4.083426892921084e-01 & -3.188313657255786e-02 & -5.078484494982506e-02 \\ -5.405253872719874e-02 & 5.983297027359225e-01 & -2.567581001370201e-01 \\ -2.861544279518418e-02 & -2.124192958277383e-01 & 6.048650902906697e-01 \end{bmatrix}$$

$$\widetilde{A}_{(1,0)} = \begin{bmatrix} -1.655461990047816e-01 & -1.558821141791788e-01 & -1.558821141791788e-01 \\ 1.541765874068727e-01 & 1.661307926654759e-01 & 1.004418790233459e-01 \\ 1.541765874068727e-01 & 1.004418790233459e-01 & 1.661307926654759e-01 \end{bmatrix}$$

$$\widetilde{A}_{(2,0)} = \begin{bmatrix} -4.141873962772590e-02 & 6.193084283933032e-04 & 6.193084283933032e-04 \\ 2.627238299781715e-02 & -1.027319934536386e-03 & -2.058238042526939e-02 \\ 2.627238299781715e-02 & -2.058238042526939e-02 & -1.027319934536386e-03 \end{bmatrix}$$

$$\widetilde{A}_{(3,0)} = \begin{bmatrix} 2.645028705212706e-01 & -3.010772608614825e-02 & -3.967598932261100e-02 \\ -2.569080244001507e-01 & 7.970072862447103e-03 & 6.204791521404297e-02 \\ -1.360002542897908e-01 & 3.742488523769980e-02 & 2.366160311200287e-03 \end{bmatrix}$$

$$\widetilde{A}_{(-2,1)} = \begin{bmatrix} 2.260542043639538e-02 & 8.003991286758694e-02 & 1.276464109542424e-01 \\ 6.170822938557453e-03 & 5.793682782654931e-03 & 2.507253131582465e-02 \\ -2.009176890381660e-02 & -4.879655861320484e-02 & -8.732934266712920e-02 \end{bmatrix}$$

$$\widetilde{A}_{(-1,1)} = \begin{bmatrix} 1.661307926654759e-01 & 1.004418790233459e-01 & 1.541765874068727e-01 \\ 1.004418790233459e-01 & 1.661307926654759e-01 & 1.541765874068727e-01 \\ -1.558821141791788e-01 & -1.558821141791788e-01 & -1.655461990047816e-01 \end{bmatrix}$$

$$\widetilde{A}_{(0,1)} = \begin{bmatrix} -2.630104470330473e-02 & -5.966619549478847e-02 & -9.198995834543475e-02 \\ 2.503925060912631e-01 & 2.193174757327797e-01 & 2.503925060912631e-01 \\ -9.198995834543475e-02 & -5.966619549478847e-02 & -2.630104470330473e-02 \end{bmatrix}$$

$$\widetilde{A}_{(1,1)} = \begin{bmatrix} -8.732934266712920e-02 & -2.009176890381660e-02 & -4.879655861320484e-02 \\ 1.276464109542424e-01 & 2.260542043639538e-02 & 8.003991286758694e-02 \\ 2.507253131582465e-02 & 6.170822938557453e-03 & 5.793682782654931e-03 \end{bmatrix}$$

$$\widetilde{A}_{(-2,2)} = \begin{bmatrix} -1.027319934536386e-03 & -2.058238042526939e-02 & 2.627238299781715e-02 \\ -2.058238042526939e-02 & -1.027319934536386e-03 & 2.627238299781715e-02 \\ 6.193084283933032e-04 & 6.193084283933032e-04 & -4.141873962772590e-02 \end{bmatrix}$$

$$\widetilde{A}_{(-1,2)} = \begin{bmatrix} 5.793682782654931e-03 & 2.507253131582465e-02 & 6.170822938557453e-03 \\ -4.879655861320484e-02 & -8.732934266712920e-02 & -2.009176890381660e-02 \\ 8.003991286758694e-02 & 1.276464109542424e-01 & 2.260542043639538e-02 \end{bmatrix}$$

$$\widetilde{A}_{(0,2)} = \begin{bmatrix} -3.855405958898559e-03 & 2.033351440574390e-03 & -2.341046644963156e-02 \\ 2.768642600999824e-02 & -3.576256757900155e-02 & 2.768642600999824e-02 \\ -2.341046644963156e-02 & 2.033351440574390e-03 & -3.855405958898559e-03 \end{bmatrix}$$

$$\widetilde{A}_{(-3,3)} = \begin{bmatrix} -1.171678421738472e-02 & 7.189134375395888e-02 & -2.175343102404871e-01 \\ -7.699067774146577e-03 & 2.492813681712348e-02 & -4.575234826609804e-02 \\ 5.360479238279715e-02 & -8.153224855708370e-02 & 9.707783358337981e-02 \end{bmatrix}$$

$$\widetilde{A}_{(0,3)} = \begin{bmatrix} 1.851591042751741e-02 & -5.370310538593751e-02 & 1.147251773170392e-01 \\ -6.716926504763816e-02 & 1.099022863625919e-01 & -1.897051670693409e-01 \\ -6.335735411643897e-02 & 3.218787560125702e-02 & -1.812901060699078e-02 \end{bmatrix}$$